Mon. Not. R. Astron. Soc. **000**, 000–000 (0000) Printed 1 February 2008 (MN LATEX style file v1.4)

Projected bispectrum in spherical harmonics and its application to angular galaxy catalogues

Licia Verde[1], Alan F. Heavens[1], Sabino Matarrese[2,3]

[1] *Institute for Astronomy, University of Edinburgh, Royal Observatory, Blackford Hill, Edinburgh EH9 3HJ, United Kingdom*
[2] *Dipartimento di Fisica* Galileo Galilei, *Università di Padova, via Marzolo 8, I-35131 Padova, Italy*
[3] *Max-Planck-Institut für Astrophysik, Karl-Schwarzschild-Strasse 1, D-85748 Garching, Germany.*

arXiv:astro-ph/0002240v2 22 Jun 2000

1 February 2008

ABSTRACT

We present a theoretical and exact analysis of the bispectrum of projected galaxy catalogues. The result can be generalized to evaluate the projection in spherical harmonics of any 3D bispectrum and therefore has applications to cosmic microwave background and gravitational lensing studies.

By expanding the 2D distribution of galaxies on the sky in spherical harmonics, we show how the 3-point function of the coefficients can be used in principle to determine the bias parameter of the galaxy sample. If this can be achieved, it would allow a lifting of the degeneracy between the bias and the matter density parameter of the Universe which occurs in linear analysis of 3D galaxy catalogues. In previous papers we have shown how a similar analysis can be done in three dimensions, and we show here through an error analysis and by implementing the method on a simulated projected catalogue that ongoing three-dimensional galaxy redshift surveys (even with all the additional uncertainties introduced by partial sky coverage, redshift-space distortions and smaller numbers) will do far better than all-sky projected catalogues with similar selection function.

Key words: cosmology: theory - galaxies: clustering - bias - large-scale structure of the Universe

1 INTRODUCTION

The clustering of mass in the Universe is an important fossil record of the early perturbations which gave rise to large-scale structure today. Knowledge of the mass clustering puts powerful constraints on the quantity and properties of dark matter in the Universe, and the generation mechanism for the perturbations. Most of our knowledge of the mass clustering is, however, indirect, coming principally from the distribution of galaxies. A major obstacle in interpretation is therefore the uncertain relationship between galaxy and mass clustering - a relationship which is conventionally quantified by the 'bias parameter', b. In particular, attempts based on linear perturbation theory to measure the density parameter of the Universe, Ω_0, through peculiar velocity or redshift-distortion studies, yield only the degenerate combination $\beta = \Omega_0^{0.6}/b$, making it impossible to determine Ω_0 without determining b. The degeneracy can be lifted by going to second order in perturbation theory, and this can be achieved most elegantly by studying the bispectrum, which is the three-point function in Fourier (or spherical harmonic) space. A major positive feature of the bispectrum method is that it can provide error bars on the desired parameters. The method works because gravitational instability leads to a density field which is progressively more skewed to high densities as it develops, and this skewness appears as a non-zero bispectrum. This behaviour can also be mimicked by biasing, if the galaxy density field is a local, nonlinear function of the underlying mass density field. This possibility must be dealt with. The two effects can, however, be separated by the use of information about the shape of the structures: in essence the effect of biasing is to shift iso-density contours up (or down), while maintaining the shape of the contour; gravitational evolution, instead, changes the shape, usually leading to flattening of collapsing structures (e.g. Zel'dovich pancakes).

Fry (1994) recognized the role the bispectrum could play in determining the bias parameter, and Matarrese, Verde & Heavens (1997) (hereafter MVH97) and Verde et al. (1998) have turned the idea into a practical proposition for 3D galaxy redshift surveys by including analysis of selection functions, shot noise, and redshift distortions (see also Scoccimarro,

© 0000 RAS

Couchman & Frieman 1999). The latter is potentially a serious problem for 3D surveys, as the signal for bias comes from mildly nonlinear scales, where the redshift distortions are not trivial to analyze. However, experiments on simulated catalogues (Verde et al. 1998) show that the method is successful. Note however that the theory has been developed only in the 'distant-observer approximation' (see e.g. Kaiser 1992), and is applicable to relatively deep surveys such as the Anglo-Australian two-degree field galaxy redshift survey (Colless 1996; Colless 1999) and the Sloan Digital Sky Survey (Gunn 1995). Shallow surveys such as the IRAS PSCz should be analysed in spherical coordinates (cf Taylor & Heavens 1995; Tadros et al. 1999 for the power spectrum), and suffer from high shot noise, so cannot be usefully used for bispectrum analysis based on a Fourier expansion (see also Bharadwaj 1999).

The absence of suitable existing 3D surveys prompts us to consider whether the bias might be extracted from a projected galaxy catalogue, such as the APM galaxy survey (Maddox et al. 1990; Loveday et al. 1992; Loveday 1996). With only angular positions, the information is more limited, but the survey is not complicated by redshift distortions, and contains a large number $\sim 10^6$ of galaxies. The DPOSS catalogue (Djorgovski et al. 1998) will be even larger, with 50 million galaxies and nearly all-sky. There are two important caveats to keep in mind: first, to have a measurement of Ω_0 we need to be able to measure the β parameter and the linear bias parameter. It is not possible to extract the β parameter from a two-dimensional survey, β will need to be determined from a -*different*- three-dimensional survey. The selection criteria will necessarily be different for different catalogues, and so will be the galaxy population selected. Since different galaxy populations can have different bias with respect to the underlying dark matter distribution, some care needs to be taken in the interpretation of the final result i.e. the value for Ω_0. The other caveat concerns the effect of the evolution along the line of sight (also referred to as the *light-cone effect*). This is due to the fact that galaxy clustering evolves gravitationally with time along the line of sight and depends on the (unknown) cosmology. For shallow surveys such as the APM, this effect is smaller or comparable to the cosmic variance, in what follows we will neglect this effect for this reason. However, for deeper surveys, this effect needs to be properly taken into account. Assuming these issues can be dealt with, the key requirement is to obtain an expression for the projected bispectrum given an analytical formula for the spatial one. An expression for the projected bispectrum in the small angle approximation has been presented by Buchalter, Kamionkowski & Jaffe (1999). However this might not be a good approximation for the bispectrum if the sample is close enough to the observer or if the scales under analysis are large. In fact it is not known *a priori* whether, for the bispectrum, the small angle approximation is valid on large enough scales for the second order perturbation theory to hold: it is necessary to obtain an exact expression for the projected bispectrum using spherical harmonics expansion. Only then it will be possible to test the limit of validity for the small-angle approximation bispectrum (Verde et al. 2000).

In this paper, we develop the theory for projected catalogues in a full treatment. The resulting expression for the spherical harmonic projected bispectrum can straightforwardly be applied to gravitational lensing and to cosmic microwave background (CMB) studies, for comparison with observations such as the claimed detection by Ferreira, Magueijo & Gorski (1998).

In Section 2 we expand the sky density of galaxies in spherical harmonics with coefficients a_ℓ^m, and compute an explicit expression for the bispectrum $\langle a_{\ell_1}^{m_1} a_{\ell_2}^{m_2} a_{\ell_3}^{m_3} \rangle$ accurate to second-order in perturbation theory. In particular, we show how this quantity depends on the bias parameter. We present in Section 3 an error analysis specific to the second-order perturbation theory bispectrum, which shows the expected uncertainty in the derived bias parameter, and test on a numerical simulation. In the Appendices, we detail asymptotic results which are useful for high-ℓ spherical harmonics. The main conclusion of large-scale structure application in this paper is that 3D large scale structure surveys (even with small sky coverage, smaller numbers, and the complications of redshift-space distortion, shot noise etc.) will do far better than all-sky projected catalogues for the purpose of measuring the bias parameter. However the mathematics developed for this purpose has much wider applications: with appropriate radial weight functions, the analysis can be applied to the CMB bispectrum induced by lensing, Sunyaev-Zel'dovich effect, the integrated Sachs-Wolfe effect or foreground point sources, and to gravitational lenses studies.

2 PROJECTED BISPECTRUM IN SPHERICAL HARMONICS

Let the projected galaxy density field be $n(\Omega)$, where Ω represents angular positions in the sky. If the three-dimensional galaxy density field is $\rho(\mathbf{r})$ (with mean $\overline{\rho}$) and the selection function is $\psi(r)$, the projected density is

$$n(\Omega)d\Omega = \left(\int dr\, r^2 \rho(\mathbf{r}) \psi(r) \right) d\Omega. \tag{1}$$

We expand the projected density in spherical harmonics (see Appendix A for definitions)

$$\begin{aligned} a_\ell^m &\equiv \frac{1}{\overline{n}} \int d\Omega\, n(\Omega) Y_\ell^{\,m}(\Omega) \\ &= \frac{\overline{\rho}}{\overline{n}} \int d\Omega dr\, r^2 \delta(r) \psi(r) Y_\ell^{\,m}(\Omega) \text{ for } \ell \neq 0 \end{aligned} \tag{2}$$

where $\delta \equiv (\rho - \overline{\rho})/\overline{\rho}$ is the fractional overdensity in galaxies. The average surface density is

$$\overline{n} = \int dr\, r^2 \overline{\rho}\psi(r). \tag{3}$$

and is inserted in the transform for convenience. The three-point function of the coefficients may be factorised by isotropy (e.g. Luo 1994) into

$$\langle a_{\ell_1}^{m_1} a_{\ell_2}^{m_2} a_{\ell_3}^{m_3} \rangle = B_{\ell_1\ell_2\ell_3} \begin{pmatrix} \ell_1 & \ell_2 & \ell_3 \\ m_1 & m_2 & m_3 \end{pmatrix} \tag{4}$$

where $\begin{pmatrix} \ell_1 & \ell_2 & \ell_3 \\ m_1 & m_2 & m_3 \end{pmatrix}$ is the Wigner 3J symbol. We refer to $B_{\ell_1\ell_2\ell_3}$ as the angular bispectrum. From general considerations about rotational invariance of the quantity $\langle a_{\ell_1}^{m_1} a_{\ell_2}^{m_2} a_{\ell_3}^{m_3} \rangle$ the indices ℓ_i, m_i for $i = 1, 2, 3$ must satisfy the following conditions:

(i) $\ell_j + \ell_k \geq \ell_1 \geq \mid \ell_j - \ell_k \mid$ (triangle rule)
(ii) $\ell_1 + \ell_2 + \ell_3 =$ even
(iii) $m_1 + m_2 + m_3 = 0$.

The presence of the 3J symbol ensures that these conditions are satisfied.

In order to be able to extract the bias parameter from projected catalogues, the effect of the projection in the configuration dependence of the bispectrum needs to be understood (Fry & Thomas 1999).

To do so, we compute the angular bispectrum in terms of the 3D bispectrum, $B(\mathbf{k}_1, \mathbf{k}_2, \mathbf{k}_3)$ defined by $\langle \delta_{\mathbf{k}1} \delta_{\mathbf{k}2} \delta_{\mathbf{k}3} \rangle = (2\pi)^3 B(\mathbf{k}_1, \mathbf{k}_2, \mathbf{k}_3) \delta^D(\mathbf{k}_1 + \mathbf{k}_2 + \mathbf{k}_3)$, where the Fourier transform of δ is $\delta_{\mathbf{k}} \equiv \int d^3\mathbf{r}\ \delta(\mathbf{r}) \exp(i\mathbf{k}\cdot\mathbf{r})$, and δ^D denotes the Dirac delta function.

We proceed from (2):

$$\langle a_{\ell_1}^{m_1} a_{\ell_2}^{m_2} a_{\ell_3}^{m_3} \rangle = \left(\frac{\overline{\rho}}{\overline{n}}\right)^3 \int d\Omega_1 d\Omega_2 d\Omega_3 dr_1 dr_2 dr_3 r_1^2 r_2^2 r_3^2 \psi_1\psi_2\psi_3 \langle \delta(\mathbf{r}_1)\delta(\mathbf{r}_2)\delta(\mathbf{r}_3)\rangle Y_{\ell_1}^{m_1}(\Omega_1) Y_{\ell_2}^{m_2}(\Omega_2) Y_{\ell_3}^{m_3}(\Omega_3)\ . \tag{5}$$

The 3D three-point function (in real space) is related to the 3D bispectrum by

$$\langle \delta(\mathbf{r}_1)\delta(\mathbf{r}_2)\delta(\mathbf{r}_3)\rangle = \frac{1}{(2\pi)^6} \int d^3\mathbf{k}_1 d^3\mathbf{k}_2 d^3\mathbf{k}_3 B(\mathbf{k}_1, \mathbf{k}_2, \mathbf{k}_3) e^{i(\mathbf{k}_1\cdot\mathbf{r}_1 + \mathbf{k}_2\cdot\mathbf{r}_2 + \mathbf{k}_3\cdot\mathbf{r}_3)} \delta^D(\mathbf{k}_1 + \mathbf{k}_2 + \mathbf{k}_3)\ . \tag{6}$$

We then define the quantity:

$$I(\mathbf{r}_1, \mathbf{r}_2, \mathbf{r}_3) \equiv \int_0^\infty dk_1 dk_2 dk_3 k_1^2 k_2^2 k_3^2 \int_{4\pi} d\Omega_{k_1} d\Omega_{k_2} d\Omega_{k_3} B(\mathbf{k_1}, \mathbf{k_2}, \mathbf{k_3}) e^{i(\mathbf{k_1}\cdot\mathbf{r}_1 + \mathbf{k_2}\cdot\mathbf{r}_2 + \mathbf{k_3}\cdot\mathbf{r}_3)} \delta^D(\mathbf{k_1} + \mathbf{k_2} + \mathbf{k_3}) \tag{7}$$

because we will later expand the exponential in spherical harmonics and perform the angular integrations in (7) explicitly.

In second order perturbation theory the bispectrum is:

$$B(\mathbf{k_1}, \mathbf{k_2}, \mathbf{k_3}) = \mathcal{K}(\mathbf{k_1}, \mathbf{k_2}) P(k_1) P(k_2) + cyc.\ , \tag{8}$$

where the shape-dependent factors $\mathcal{K}$ can be found in Fry (1984), Catelan et al. (1995) and MVH97. The dependence of $\mathcal{K}$ on the cosmology in negligible (e.g. Kamionkowski & Buchalter (1999) and references therein), so in what follows we assume an Einstein-de Sitter Universe. The factors are, however, dependent on the biasing model assumed. If we take a local biasing model, then for consistency with second-order perturbation theory, we expand in a Taylor series the galaxy overdensity to second-order in the matter overdensity δ_m:

$$\delta(\mathbf{x}) = b_1 \delta_m(\mathbf{x}) + \frac{1}{2} b_2 \delta_m(\mathbf{x})^2, \tag{9}$$

(a constant term b_0 is irrelevant except at $\mathbf{k} = \mathbf{0}$ and is ignored). Here b_1 is the linear bias parameter and b_2 is the quadratic bias parameter. The linear bias parameter b that appears in the definition of β and that is needed to recover Ω_0, is $b = b_1$ on large scales, under fairly general conditions (Heavens, Matarrese & Verde 1998). Note that we take the bias function to be deterministic, not stochastic (cf Cen & Ostriker 1992; Dekel & Lahav 1999; Tegmark & Bromley 1999; Matsubara 1999; Somerville et al. 1999); it has been shown (Taruya, Koyama & Soda 1999) that the effect of stochastic bias on the bispectrum is very similar to that of nonlinear bias (Eq. 9). This formalism might be straightforwardly extended to the case when the bias process operates in Lagrangian, rather than Eulerian, space (Catelan et al. 1998).

With these assumptions, a typical cyclical term can be written

$$\mathcal{K}(\mathbf{k_1}, \mathbf{k_2}) = A_0 + A_1 \cos(\theta_{12}) + A_2 \cos^2(\theta_{12}) \tag{10}$$

where θ_{12} denotes the angle between $\mathbf{k_1}$ and $\mathbf{k_2}$, and

$$\begin{aligned} A_0 &= \frac{10}{7} c_1 + c_2 \\ A_1 &= c_1 \left(\frac{k_1}{k_2} + \frac{k_2}{k_1}\right) \\ A_2 &= \frac{4}{7} c_1, \end{aligned} \tag{11}$$

and $c_1 = 1/b_1$; $c_2 = b_2/b_1^2$. Through these relations, the projected bispectrum will depend on the bias parameters b_1 and b_2.

Using this, we will now calculate the theoretical expression for the projected bispectrum in spherical harmonics in the mildly nonlinear regime. With substitution (8) we find

$$I(\mathbf{r}_1, \mathbf{r}_2, \mathbf{r}_3) \equiv I_{12} + I_{23} + I_{13} \tag{12}$$

Using the properties of spherical harmonics in Appendix A [equation (46), the orthogonality relation, (41) and (44)], we obtain that a typical cyclical term is:

$$\begin{aligned} I_{12} &= (4\pi)^4 \int_0^\infty d^3\mathbf{k}_1 d^3\mathbf{k}_2 \mathcal{K}(\mathbf{k}_1, \mathbf{k}_2) P(k_1) P(k_2) \times \\ &\sum_{\ell_1' m_1'} i^{\ell_1'} j_{\ell_1'}(k_1 r_1) Y^{*m_1'}_{\ell_1'}(\Omega_{k_1}) Y^{m_1'}_{\ell_1'}(\Omega_{r_1}) \sum_{\ell_2' m_2'} i^{\ell_2'} j_{\ell_2'}(k_2 r_2) Y^{*m_2'}_{\ell_2'}(\Omega_{k_2}) Y^{m_2'}_{\ell_2'}(\Omega_{r_2}) \times \\ &\sum_{L_1 n_1} i^{L_1} j_{L_1}(k_1 r_3) Y^{*n_1}_{L_1}(-\Omega_{k_1}) Y^{n_1}_{L_1}(\Omega_{r_3}) \sum_{L_2 n_2} i^{L_2} j_{L_2}(k_2 r_3) Y^{*n_2}_{L_2}(-\Omega_{k_2}) Y^{n_2}_{L_2}(\Omega_{r_3}). \end{aligned} \tag{13}$$

We can now write

$$\int_{4\pi} d\Omega Y^{*m_1}_{\ell_1}(\Omega) Y^{m_2}_{\ell_2}(\Omega) Y^{m_3}_{\ell_3}(\Omega) = \mathcal{H}^{m_1 m_2 m_3}_{\ell_1\, \ell_2\, \ell_3} \ , \tag{14}$$

which can be expressed in term of Clebsch-Gordan coefficients, and is non-zero only if the following symmetry conditions are satisfied:

- $m_2 + m_3 = m_1$
- $\ell_1 + \ell_2 + \ell_3 =$ even
- ℓ_1, ℓ_2, ℓ_3 satisfy the triangle rule

From equation (13) we thus obtain:

$$\int_{4\pi} d\Omega_{r_1} d\Omega_{r_2} d\Omega_{r_3} Y^{m_1}_{\ell_1}(\Omega_{r_1}) Y^{m_2}_{\ell_2}(\Omega_{r_2}) Y^{m_3}_{\ell_3}(\Omega_{r_3}) I_{12} = (4\pi)^4 \int dk_1 dk_2 k_1^2 k_2^2 P(k_1) P(k_2) F(r_1, r_2, r_3, k_1, k_2) \ , \tag{15}$$

where

$$\begin{aligned} F(r_1, r_2, r_3, k_1, k_2) &= \int d\Omega_{k_1} d\Omega_{k_2} \left(A_0 + A_1 \cos\theta_{12} + A_2 \cos^2\theta_{12}\right) i^{\ell_1 + \ell_2} (-1)^{(m_1 + m_2 + m_3)} j_{\ell_1}(k_1 r_1) j_{\ell_2}(k_2 r_2) \times \\ &\sum_{\ell_{6,7} m_{6,7}} i^{\ell_6 + \ell_7} j_{\ell_6}(k_1 r_3) j_{\ell_7}(k_2 r_3) Y^{*-m_1}_{\ell_1}(\Omega_{k_1}) Y^{*-m_2}_{\ell_2}(\Omega_{k_2}) Y^{*m_6}_{\ell_6}(-\Omega_{k_1}) Y^{*m_7}_{\ell_7}(-\Omega_{k_2}) \mathcal{H}^{-m_3 m_6 m_7}_{\ell_3\, \ell_6\, \ell_7} \end{aligned} \tag{16}$$

and F can be written as $F_0 + F_1 + F_2$ where F_0 involves the term A_0 etc.

The F_0 term is easily calculated:

$$F_0 = A_0 i^{2(\ell_1 + \ell_2)} j_{\ell_1}(k_1 r_1) j_{\ell_2}(k_2 r_2) j_{\ell_1}(k_1 r_3) j_{\ell_2}(k_2 r_3) \mathcal{H}^{-m_3 m_1 m_2}_{\ell_3\, \ell_1\, \ell_2} \tag{17}$$

and therefore satisfies the symmetry rules.

For F_1 and F_2 we exploit the fact that:

$$\cos\theta_{12} = P_1(\cos\theta_{12}), \tag{18}$$

$$\cos^2\theta_{12} = \frac{1}{3}\left[2P_2(\cos\theta_{12}) + P_0(\cos\theta_{12})\right] \tag{19}$$

and use the addition theorem for spherical harmonics:

$$P_n(\cos\theta_{12}) = \frac{4\pi}{2n+1} \sum_{m=-n}^{n} Y^m_n(\Omega_{k_1}) Y^{*m}_n(\Omega_{k_2}). \tag{20}$$

The F_1 term then becomes:

$$F_1 = A_1 \frac{4\pi}{3} i^{\ell_1 + \ell_2} (-1)^{m_1 + m_3} j_{\ell_1}(k_1 r_1) j_{\ell_2}(k_2 r_2) \sum_{\ell_6 m_6 \ell_7 m_7 M} i^{\ell_6 + \ell_7} j_{\ell_6}(k_1 r_3) j_{\ell_7}(k_2 k_3) \mathcal{H}^{-m_3 m_6 m_7}_{\ell_3\, \ell_6\, \ell_7} \mathcal{H}^{-m_1 -m_6 M}_{\ell_1\, \ell_6\, 1} \mathcal{H}^{M m_2 -m_7}_{1\, \ell_2\, \ell_7}. \tag{21}$$

It is easy to see that $m_6 + m_7 = -m_3$. To demonstrate that the symmetry conditions are all satisfied, consider the following part of eq.(21):

$$\sum_{m_6 m_7 M} \mathcal{H}^{-m_3 m_6 m_7}_{\ell_3\, \ell_6\, \ell_7} \mathcal{H}^{-m_1 -m_6 M}_{\ell_1\, \ell_6\, 1} \mathcal{H}^{M m_2 -m_7}_{1\, \ell_2\, \ell_7} \ ; \tag{22}$$

let's introduce a new quantity $h^{m_1 m_2 m_3}_{\ell_1\,\ell_2\,\ell_3}$ that is symmetric for any permutation of the columns $\binom{m_i}{\ell_i}$. It is clear that:

$$\mathcal{H}^{m_1 m_2 m_3}_{\ell_1\,\ell_2\,\ell_3} = (-1)^{m_1} h^{-m_1 m_2 m_3}_{\ell_1\,\ell_2\,\ell_3}. \tag{23}$$

The quantity $h^{m_1 m_2 m_3}_{\ell_1\,\ell_2\,\ell_3}$ can be written in terms of the $3J$ symbols:

$$h^{m_1 m_2 m_3}_{\ell_1\,\ell_2\,\ell_3} = \sqrt{(2\ell_1+1)(2\ell_2+1)(2\ell_3+1)/(4\pi)}\begin{pmatrix}\ell_1 & \ell_2 & \ell_3\\ 0 & 0 & 0\end{pmatrix}\begin{pmatrix}\ell_1 & \ell_2 & \ell_3\\ m_1 & m_2 & m_3\end{pmatrix}. \tag{24}$$

Equation (21) therefore contains the following multiplicative term:

$$\sum_{m_6 m_7 M}(-1)^{-m3-m_1+M}\begin{pmatrix}\ell_3 & \ell_6 & \ell_7\\ m_3 & m_6 & m_7\end{pmatrix}\begin{pmatrix}\ell_1 & \ell_6 & 1\\ m_1 & -m_6 & M\end{pmatrix}\begin{pmatrix}1 & \ell_2 & \ell_7\\ -M & m_2 & -m_7\end{pmatrix} = (-1)^{\ell_6+\ell_7+\ell}\begin{pmatrix}\ell_1 & \ell_2 & \ell_3\\ m_1 & m_2 & m_3\end{pmatrix}\begin{Bmatrix}\ell_1 & \ell_2 & \ell_3\\ \ell_7 & \ell_6 & 1\end{Bmatrix}, \tag{25}$$

where $\begin{Bmatrix}\ell_1 & \ell_2 & \ell_3\\ \ell_7 & \ell_6 & 1\end{Bmatrix}$ denotes the 6J symbol. In the last equality we used eq. (4.88) of Sobelman (1979). The properties of the 3J symbol ensure that the F_1 term satisfies the symmetry conditions.

Similarly for the F_2 term we obtain

$$\begin{aligned} F_2 &= A_2 i^{\ell_1+\ell_2}(-1)^{m_1+m_3}\frac{4\pi}{3}j_{\ell_1}(k_1 r_1)j_{\ell_2}(k_2 r_2)\sum_{\ell_{6,7}m_{6,7}M}(-i)^{\ell_6+\ell_7}j_{\ell_6}(k_1 r_3)j_{\ell_7}(k_2 r_3)\times \\ &\quad \mathcal{H}^{-m3 m_6 m_7}_{\ell_3\ \ell_6\ \ell_7}\left[\frac{2}{5}\mathcal{H}^{-m_1 1 M-m_6}_{\ell_1\ 2\ \ell_6}\mathcal{H}^{M m_2 -m_7}_{2\ \ell_2\ \ell_7} + \mathcal{H}^{-m_1 0 -m_6}_{\ell_1\ 0\ \ell_6}\mathcal{H}^{0 m_2 -m_7}_{0\ \ell_2\ \ell_7}\right]. \end{aligned} \tag{26}$$

The second term in the square brackets does not present any problem, in fact it is nonzero only if $\ell_1 = \ell_6$, $\ell_2 = \ell_7$, $m_1 = m_6$, $m_2 = m_7$, and satisfies the symmetry conditions. Similar methods to those above complete the symmetry considerations.

Factorising the Wigner 3J symbol, and collecting terms together, we find the expression for the angular bispectrum, as a sum of cyclical permutations:

$$B_{\ell_1\ell_2\ell_3} = \mathcal{B}_{12} + \mathcal{B}_{13} + \mathcal{B}_{23} \tag{27}$$

where, writing $\Psi_\ell(k) = \overline{\rho}\int dr r^2 j_\ell(kr)\psi(r)$,

$$\begin{aligned} \mathcal{B}_{12} &= \frac{1}{\overline{n}^3}\frac{16}{\pi}\sqrt{\frac{(2\ell_1+1)(2\ell_2+1)(2\ell_3+1)}{(4\pi)^3}}\int dk_1 dk_2 i^{\ell_1+\ell_2}k_1^2 k_2^2 P(k_1)P(k_2)\Psi_{\ell_1}(k_1)\Psi_{\ell_2}(k_2)\times \\ &\quad \sum_{\ell\ell_6\ell_7} i^{\ell_6+\ell_7}(-1)^\ell B_\ell(k_1,k_2)(2\ell_6+1)(2\ell_7+1)\overline{\rho}\int dr r^2\psi(r)j_{\ell_6}(k_1 r)j_{\ell_7}(k_2 r)\begin{pmatrix}\ell_1 & \ell_6 & \ell\\ 0 & 0 & 0\end{pmatrix}\begin{pmatrix}\ell_2 & \ell_7 & \ell\\ 0 & 0 & 0\end{pmatrix}\begin{pmatrix}\ell_3 & \ell_6 & \ell_7\\ 0 & 0 & 0\end{pmatrix}\begin{Bmatrix}\ell_1 & \ell_2 & \ell_3\\ \ell_7 & \ell_6 & \ell\end{Bmatrix} \end{aligned} \tag{28}$$

where $B_\ell(k_1,k_2)$ for $\ell = 0,1,2$ are:

$$\begin{aligned} B_0(k_1,k_2) &= \frac{34}{21}c_1 + c_2 \\ B_1(k_1,k_2) &= c_1\left(\frac{k_1}{k_2}+\frac{k_2}{k_1}\right) \\ B_2(k_1,k_2) &= \frac{8}{21}c_1, \end{aligned} \tag{29}$$

and the sum $\sum_{\ell\ell_6\ell_7}$ extends over $\ell = 0,1,2$; $\ell_6 = \ell_1 - \ell.....\ell_1 + \ell$; $\ell_7 = \ell_2 - \ell.....\ell_2 + \ell$.

The above expression can easily be generalized for any 3D bispectrum. In fact, since a) the bispectrum is non-zero only if the three k vectors form a triangle, b) the bispectrum does not depend on the spatial orientation of the triangle (isotropy) and c) a triangle is completely specified only by the magnitude of two sides and the angle between them, the bispectrum can always be expressed as a sum over three cyclical terms each involving only the modulus of two k-vectors and the angle between them:

$$B(\mathbf{k}_1,\mathbf{k}_2,\mathbf{k}_3) = \mathcal{F}(k_1,k_2,\theta_{12}). \tag{30}$$

Each of the cyclical terms can therefore be expanded as:

$$\mathcal{F}(k_1,k_2,\theta_{12}) = P(k_1)P(k_2)\sum_{\ell=0}^{n}B_\ell(k_1,k_2)P_\ell(\cos\theta_{12}) \tag{31}$$

where now $P(k_i)$ is an arbitrary function of $|\mathbf{k}_i|$, the coefficients B_ℓ can depend on any combination of $|\mathbf{k}_1|$ and $|\mathbf{k}_2|$ and the sum over ℓ should in principle go to infinity, but in practice will be truncated at n.

We find that the exact expression for the projected bispectrum $B_{\ell_1\ell_2\ell_3}$ is still given by equations (27) and (28) where now the sum over ℓ goes up to n.

This, with equations (27) and (28), is the major new result of this paper.

2.1 Applications

Equation (28) has therefore much wider applications than the second-order gravitationally induced bispectrum considered so far. The mathematics developed for this purpose can be straightforwardly applied to CMB and gravitational lensing studies. The gravitational fluctuations and cosmological structures along the path of the last-scattering surface photons. distort the CMB signal mainly through gravitational lensing, the integrated Sachs-Wolfe effect (Sachs & Wolfe 1967), the Sunyaev-Zel'dovich effect (Sunyaev & Zel'dovich 1980), and through the Rees-Sciama effect (Rees & Sciama 1968) and other second order effects (e.g. Mollerach & Matarrese 1997 and references therein). In particular, if the primordial fluctuations were Gaussian, many of these effects can introduce non gaussian features in the CMB signal. The bispectrum is a powerful tool for detecting these effects to probe the low-redshift Universe (Goldberg & Spergel 1998, Spergel & Goldberg 1998). Contributions to the CMB bispectrum induced by secondary anisotropies during reionization (Cooray & Hu 1999), non-linear gravitational evolution (Luo & Schramm 1994; Mollerach et al. 1995; Munshi, Souradeep & Starobinsky 1995) and foregrounds (e.g. Refregier, Spergel & Herbig 1998) imprint specific signatures on the CMB bispectrum which need to be subtracted from the signal in order to be able to test the gaussian nature of primordial fluctuations.

On the other hand, primordial fluctuations can induce nonzero bispectrum in the CMB, that encloses information about the physical mechanism that generated them (e.g. Falk, Rangarajan & Srednicki 1993; Luo & Schramm 1994, Gangui et al. 1994, Mollerach et al. 1995, Gangui & Mollerach 1996, Wang & Kamionkowski 1999, Gangui & Martin 1999). The evaluation of all these contributions to the observed CMB bispectrum requires calculation of an integral as in our equation (5) and (6), where $r^2\psi(r)$ is replaced by an appropriate weight function.

In the local Universe, gravitational lensing provides a direct probe of the mass fluctuations. The study of Fourier space correlation functions of the gravitational weak shear and convergence field is still in its infancy, but it is potentially fruitful: it could give us detailed knowledge of the correlation properties of the projected mass distribution (e.g. Bernardeau et al. 1997 and references therein, Munshi 2000).

In the present paper we will use equation (28) together with (27) as an *exact* expression for the second-order perturbation theory bispectrum of an angular catalogue with selection function $\psi(r)$ and galaxy power spectrum $P(k)$, assuming a local bias model with parameters b_1 and b_2. In principle, one can estimate the angular bispectrum from a projected galaxy catalogue, and use likelihood methods to constrain the bias parameters, which enter through the B_ℓ terms. In Section 3, we compute the likely errors from such a study, to determine if it is worthwhile to undertake such an analysis with current catalogues. Before we do so, it is worth noting that, in the current form, it is very expensive to compute: in the following subsection we rewrite it in a form more suitable for practical evaluation.

2.2 Practical evaluation of $B_{\ell_1\ell_2\ell_3}$

From a computational point of view it is possible to speed up the calculations considerably (and consequently make the problem computationally manageable) by rewriting equation (28) in terms of the function Θ^q_ℓ defined as:

$$\Theta^q_{\ell_i}(\ell_j, r) \equiv \int dk \Psi_{\ell_i}(k) k^2 P(k) j_{\ell_j}(kr) k^q \tag{32}$$

where $q = -1, 0, 1$ and $\{i, j\} = \{1, 6\}$ or $\{2, 7\}$. This function can be evaluated and tabulated in advance to speed up the analysis. With this definition, we can write the components of the angular bispectrum as

$$\begin{aligned}
\mathcal{B}_{12} \;=\; & \frac{1}{\overline{n}^3}\frac{16}{\pi}\sqrt{\frac{(2\ell_1+1)(2\ell_2+1)(2\ell_3+1)}{(4\pi)^3}} i^{\ell_1+\ell_2} \times \\
& \int dr_3 r_3^2 \psi(r_3) \left(\frac{34}{21}c_1 + c_2\right) \Theta^0_{\ell_1}(\ell_1, r_3)\Theta^0_{\ell_2}(\ell_2, r_3) \begin{pmatrix} \ell_1 & \ell_1 & 0 \\ 0 & 0 & 0 \end{pmatrix} \begin{pmatrix} \ell_2 & \ell_2 & 0 \\ 0 & 0 & 0 \end{pmatrix} \begin{pmatrix} \ell_3 & \ell_1 & \ell_2 \\ 0 & 0 & 0 \end{pmatrix} \begin{Bmatrix} \ell_1 & \ell_2 & \ell_3 \\ \ell_1 & \ell_2 & 0 \end{Bmatrix} + \\
& c_1 \sum_{\substack{\ell_1-1<\ell_6<\ell_1+1 \\ \ell_2-1<\ell_7<\ell_2+1}} \left[\Theta^{-1}_{\ell_1}(\ell_6, r_3)\Theta^{+1}_{\ell_2}(\ell_7, r_3) + \Theta^{+1}_{\ell_1}(\ell_6, r_3)\Theta^{-1}_{\ell_2}(\ell_7, r_3)\right] \begin{pmatrix} \ell_1 & \ell_6 & \ell \\ 0 & 0 & 0 \end{pmatrix} \begin{pmatrix} \ell_2 & \ell_7 & \ell \\ 0 & 0 & 0 \end{pmatrix} \begin{pmatrix} \ell_3 & \ell_6 & \ell_7 \\ 0 & 0 & 0 \end{pmatrix} \begin{Bmatrix} \ell_1 & \ell_2 & \ell_3 \\ \ell_7 & \ell_6 & \ell \end{Bmatrix} + \\
& \frac{8}{21}c_1 \sum_{\substack{\ell_1-2<\ell_6<\ell_1+2 \\ \ell_2-2<\ell_7<\ell_2+2}} \Theta^0_{\ell_1}(\ell_6, r_3)\Theta^0_{\ell_2}(\ell_7, r_3) \begin{pmatrix} \ell_1 & \ell_6 & \ell \\ 0 & 0 & 0 \end{pmatrix} \begin{pmatrix} \ell_2 & \ell_7 & \ell \\ 0 & 0 & 0 \end{pmatrix} \begin{pmatrix} \ell_3 & \ell_6 & \ell_7 \\ 0 & 0 & 0 \end{pmatrix} \begin{Bmatrix} \ell_1 & \ell_2 & \ell_3 \\ \ell_7 & \ell_6 & \ell \end{Bmatrix}.
\end{aligned} \tag{33}$$

Note that this analysis is appropriate for all-sky coverage, and ignores shot noise. This is a good approximation for the high surface-density catalogues such as APM, in the range where perturbation theory is valid. Estimators for noisy data and partial sky coverage are presented in Heavens (1998) and Heavens (2000), see also Gangui & Martin (2000). Note also that numerical codes can run into difficulties when computing the spherical harmonic expansion and 3J symbols for high ℓ. In Appendix C we give asymptotic expressions at high ℓ for the 3J symbols that are easily evaluated, and we present a way to calculate spherical harmonics fast and accurately at high ℓ.

3 ERROR ANALYSIS FOR THE BIAS PARAMETER

The spherical harmonic bispectrum in second-order perturbation theory is a known function of the galaxy power spectrum, and depends on the bias parameters b_1 and b_2 through B_0, B_1, B_2 (equation 29). Equation (28) relates therefore two measurable quantities (the spherical harmonic bispectrum of galaxies and the galaxy power spectrum) via the unknown bias parameters b_1 and b_2. The 3D power spectrum may be obtained from the projected catalogue either by deconvolution of the angular correlation function or the angular power spectrum (e.g. Baugh & Efstathiou 1993; Baugh & Efstathiou 1994). In practice this is done in the small-angle approximation. In Appendix B we show that this is perfectly adequate for the power spectrum. We therefore have a full prescription for the angular bispectrum in terms of observable quantities and parameters which we wish to measure [equation (28) or the computationally manageable equation (33)]. The problem is therefore suitable for a likelihood analysis to extract the bias parameter. Such a programme is a major undertaking, so it makes sense to compute the expected error on the bias parameter first, to see whether the programme is likely to succeed.

3.1 Likelihood analysis for c_1 and c_2

We assume we have full sky coverage unless otherwise stated. We define the quantity[⋆] d_α=**Re**$[a_{\ell_1}^{m_1} a_{\ell_2}^{m_2} a_{\ell_3}^{m_3}]$ with ℓ_i, m_i such that $\left(\begin{smallmatrix}\ell_1 & \ell_2 & \ell_3\\ m_1 & m_2 & m_3\end{smallmatrix}\right) \neq 0$. For a given triplet ℓ_1, ℓ_2, ℓ_3 there are $(2\ell_1+1)(2\ell_2+1)$ distinct d_α. From d_α we can build the unbiased estimator of $B_{\ell_1\ell_2\ell_3}$, $\hat{D}_\alpha = \frac{d_\alpha}{\left(\begin{smallmatrix}\ell_1 & \ell_2 & \ell_3\\ m_1 & m_2 & m_3\end{smallmatrix}\right)}$.

Since $\hat{D}_\alpha$ is unbiased, any combination $D_\alpha = (\sum_{\alpha'} w_{\alpha'} \hat{D}_{\alpha'})/(\sum_{\alpha'} w_{\alpha'})$, where $w_{\alpha'}$ is a weight, is also an unbiased estimator of $B_{\ell_1\ell_2\ell_3}$.

The optimum weight w_α that minimizes the variance $\langle (D_\alpha - B_{\ell_1\,\ell_2\,\ell_3})^2 \rangle$ is $w_\alpha = 1/\sigma^2_{\hat{D}_\alpha} = \left(\begin{smallmatrix}\ell_1 & \ell_2 & \ell_3\\ m_1 & m_2 & m_3\end{smallmatrix}\right)^2 / \sigma^2_{d_\alpha}$ (cf Gangui & Martin 2000). The minimum variance estimator is

$$D_\alpha = \frac{\sum_{m_1 m_2 m_3} \frac{\left(\begin{smallmatrix}\ell_1 & \ell_2 & \ell_3\\ m_1 & m_2 & m_3\end{smallmatrix}\right) d_\alpha}{\sigma^2_{d_\alpha}}}{\sum_{m_1 m_2 m_3} \frac{\left(\begin{smallmatrix}\ell_1 & \ell_2 & \ell_3\\ m_1 & m_2 & m_3\end{smallmatrix}\right)^2}{\sigma^2_{d_\alpha}}} \tag{34}$$

The variance of d_α does depend on m, but only weakly. There is a leading term, independent of m, proportional to 3 angular power spectra ($C_{\ell_1} C_{\ell_2} C_{\ell_3}$), plus a sub-leading term proportional to $B_{\ell_i\ell_j\ell_k} B_{\ell_p\ell_q\ell_r} \left(\begin{smallmatrix}\ell_i & \ell_j & \ell_k\\ m_i & m_j & m_k\end{smallmatrix}\right) \left(\begin{smallmatrix}\ell_p & \ell_q & \ell_r\\ m_p & m_q & m_r\end{smallmatrix}\right)$, where $\{i,j,k,p,q,r\}$ is a permutation of $\{1,2,3,1,2,3\}$. If we ignore the m-dependence of this last term, then the estimator simplifies to

$$D_\alpha = \sum_{m_i} d_\alpha \left(\begin{smallmatrix}\ell_1 & \ell_2 & \ell_3\\ m_1 & m_2 & m_3\end{smallmatrix}\right), \; i = 1,2,3. \tag{35}$$

Strictly it is not the minimum variance estimator, but it is not far from it, is much simpler, and is unbiased.

3.2 A priori error for the bias parameter

Since the quantity $\langle a_{\ell_1}^{m_1} a_{\ell_2}^{m_2} a_{\ell_3}^{m_3} \rangle$ can be factorized as in equation (4) it is possible to evaluate the expected error on c_1 estimation by approximating the variance by its leading term, neglecting shot noise and by considering uncorrelated data, obtaining:

$$\sigma_{c_1}^{-2} = -\langle \frac{\partial^2 \mathcal{L}}{\partial c_1^2} \rangle \simeq \sum_{\ell_i} \frac{B^2_{\ell_1\ell_2\ell_3}}{C_{\ell_1} C_{\ell_2} C_{\ell_3}} \sum_{m_i} \frac{\left(\begin{smallmatrix}\ell_1 & \ell_2 & \ell_3\\ m_1 & m_2 & m_3\end{smallmatrix}\right)^2}{N_{\ell_i}(m_i)} \tag{36}$$

where $\mathcal{L}$ denotes the likelihood function.

The quantity $N_{\ell_i}(m_i)$ denotes the number of terms like $C_{\ell_1} C_{\ell_2} C_{\ell_3}$ present in the covariance. It depends on the configuration i.e. on the choice of the triplets of ℓ's. It is useful to notice here that in the absence of $N_{\ell_i}(m_i)$ we have

$$\sum_{m_1 m_2 m_3} \left(\begin{smallmatrix}\ell_1 & \ell_2 & \ell_3\\ m_1 & m_2 & m_3\end{smallmatrix}\right)^2 = 1. \tag{37}$$

Equation (36) assumes that the covariance matrix is diagonal, this means that different bispectrum estimators $\langle a_{\ell_1}^{m_1} a_{\ell_2}^{m_2} a_{\ell_3}^{m_3} \rangle$ are uncorrelated. In the case of a survey with full sky coverage, similarly to the three-dimensional case treated in MVH97, the covariance matrix is well approximated by a diagonal matrix if each a_ℓ^m appears in one estimator only. However, in the presence of a mask, different a_ℓ^m are correlated, therefore (36) might no longer be valid.

[⋆] **Re**[x] denotes the real part of the complex number x.

For an order-of-magnitude estimation of the expected error on the bias parameter, let us consider only equilateral configurations (i.e. configurations where $\ell_1 = \ell_2 = \ell_3$), and assume full sky coverage for a survey with the APM selection function. It is easy to estimate the error achievable on c_1 using equation (36) and considering that second order perturbation theory should hold up to $\ell = 35$. This choice is justified by the following argument: in the three-dimensional galaxy distribution, second-order perturbation theory breaks down at $k \sim 0.6$ (Mpc $h^{-1})^{-1}$ (cf MVH97, although it depends on the power spectrum slope and can be smaller, see e.g. Scoccimarro et al. (1998)) that corresponds to a scale of the order of 10 Mpc h^{-1}. At the medium depth of the APM survey (335 Mpc h^{-1}), this subtends an angle of about 0.03 radians (in agreement with the findings of Gaztanaga & Bernardeau 1998), corresponding with $\ell \sim 33$. This order of magnitude calculation yields an estimate for the error on c_1 of about ± 3.5, which is not really encouraging. However, this is only an order-of magnitude calculation: a more rigorous treatment is implemented in the next section.

3.3 The choice of the triplets

As already discussed in MVH97, the choice of the triplets to evaluate the bispectrum is very wide, but, speed and memory considerations force one to simplify the analysis by ensuring that the covariance matrix is diagonal, for a full sky survey, this can be achieved by ensuring that each ℓ appears only in one triplet. The choice of the ratio between the ℓ's (the shape) of a triplet, is influenced by the behavior of the bispectrum: triplets with the same shape give an almost degenerate information on c_1 and c_2, in practice each shape can constrain a linear combination of c_1 and c_2: the likelihood will be aligned along a straight line in the c_1,c_2 plane. The best choice to try to lift this additional degeneracy is to combine the likelihood for equilateral triplets ($\ell_1 = \ell_2 = \ell_3$) with the likelihood for degenerate triplets ($\ell_1 = \ell_2$ and $\ell_3 = 2\ell_1$).

3.4 Covariance

To perform a likelihood analysis we need an expression for the covariance matrix for our estimator $\widehat{B}_{\ell_1\ell_2\ell_3}$. It is easy to verify that, if each ℓ appears only in one $\widehat{B}_{\ell_1\ell_2\ell_3}$ then the $\widehat{B}_{\ell_1\ell_2\ell_3}$ are uncorrelated, that is:

$$\langle \widehat{B}_{\ell_1\ell_2\ell_3} \widehat{B}_{\ell_4\ell_5\ell_6} \rangle = \langle \widehat{B}_{\ell_1\ell_2\ell_3} \rangle \langle \widehat{B}_{\ell_4\ell_5\ell_6} \rangle \tag{38}$$

if $\ell_i \neq \ell_j$, where $i = 1, 2, 3$ and $j = 4, 5, 6$. This means that the off-diagonal terms of the covariance matrix are zero. In fact:

$$\langle \widehat{B}_{\ell_1\ell_2\ell_3} \widehat{B}_{\ell_4\ell_5\ell_6} \rangle = \sum_{m_1 m_2 m_3} \sum_{m_4 m_5 m_6} \langle a_{\ell_1}^{m_1} a_{\ell_2}^{m_2} a_{\ell_3}^{m_3} a_{\ell_4}^{m_4} a_{\ell_5}^{m_5} a_{\ell_6}^{m_6} \rangle \begin{pmatrix} \ell_1 & \ell_2 & \ell_3 \\ m_1 & m_2 & m_3 \end{pmatrix} \begin{pmatrix} \ell_4 & \ell_5 & \ell_6 \\ m_4 & m_5 & m_6 \end{pmatrix} \tag{39}$$

where we used the fact that $a_\ell^{*m} = (-1)^m a_\ell^{-m}$. Analogously to MVH97, the quantity $\langle a_{\ell_1}^{m_1} a_{\ell_2}^{m_2} a_{\ell_3}^{m_3} a_{\ell_4}^{m_4} a_{\ell_5}^{m_5} a_{\ell_6}^{m_6} \rangle$ can be split into:

a) 15 cyclical permutations of the kind $\langle a_{\ell_1}^{m_1} a_{\ell_2}^{m_2} \rangle \langle a_{\ell_3}^{m_3} a_{\ell_4}^{m_4} \rangle \langle a_{\ell_5}^{m_5} a_{\ell_6}^{m_6} \rangle$ that are all zero if $\ell_i \neq \ell_j$, where $i = 1, 2, 3$ and $j = 4, 5, 6$,

b) 1 term

$$B_{\ell_1\ell_2\ell_3} B_{\ell_4\ell_5\ell_6} \sum_{m_1 m_2 m_3} \sum_{m_4 m_5 m_6} \begin{pmatrix} \ell_1 & \ell_2 & \ell_3 \\ m_1 & m_2 & m_3 \end{pmatrix}^2 \begin{pmatrix} \ell_4 & \ell_5 & \ell_6 \\ m_4 & m_5 & m_6 \end{pmatrix}^2 = \langle \widehat{B}_{\ell_1\ell_2\ell_3} \rangle \langle \widehat{B}_{\ell_4\ell_5\ell_6} \rangle$$

c) 9 cyclical permutations of the kind:

$$B_{\ell_i \ell'_j \ell_k} B_{\ell'_i \ell_j \ell'_k} \sum_{m_i m_j m_k} \sum_{m'_i m'_j m'_k} \begin{pmatrix} \ell_i & \ell'_j & \ell_k \\ m_i & m'_j & m_k \end{pmatrix} \begin{pmatrix} \ell'_i & \ell_j & \ell'_k \\ m'_i & m_j & m'_k \end{pmatrix} \begin{pmatrix} \ell_1 & \ell_2 & \ell_3 \\ m_1 & m_2 & m_3 \end{pmatrix} \begin{pmatrix} \ell_4 & \ell_5 & \ell_6 \\ m_4 & m_5 & m_6 \end{pmatrix}$$

where i, j, k is any permutation of 1,2,3 and $i'j'k'$ denotes any permutation of 4,5,6. These terms in c) are all zero unless there are repeated ℓ in two different D_α.

The term in b) cancels when subtracting the mean to obtain the covariance. Let us now consider the diagonal terms of the covariance matrix: these are given by equation (39) with the following identities for the indices: 1 = 4, 2 = 5, 3 = 6. For symmetry considerations we can restrict ourselves to consider $\ell_1 \leq \ell_2 \leq \ell_3$. In the case where $\ell_1 < \ell_2 < \ell_3$ we have:

in a) only one term surviving, giving $C_{\ell_1} C_{\ell_2} C_{\ell_3}$.
in c) using (65), $3B^2_{\ell_1\ell_2\ell_3}$

In the case where $\ell_1 = \ell_2 < \ell_3$ we have:

in a) $C^2_{\ell_1} C_{\ell_3} \left[2 + \sum_{mm'} \begin{pmatrix} \ell_1 & \ell_1 & \ell_3 \\ m & -m & 0 \end{pmatrix} \begin{pmatrix} \ell_1 & \ell_1 & \ell_3 \\ m' & -m' & 0 \end{pmatrix} \right]$ in the particular case where $\ell_3 = 2\ell_1$ (degenerate configurations) as shown in Appendix C (eq. 62) we obtain to very good approximation: $C^2_{\ell_1} C_{\ell_3} \left[2 + \sqrt{(2\pi\ell_1)}/(1 + 4\ell_1) \right]$

in c) $5B^2_{\ell_1\ell_1\ell_3}$

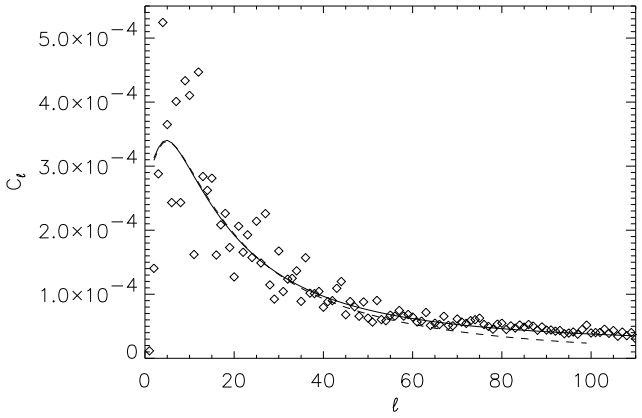

Figure 1. The power spectrum in spherical harmonics for the simulated projected catalogue. The points are the C_ℓ measured for the catalogue, the solid line is the underlying power spectrum, and the dashed line is the underlying linear power spectrum. The underlying power spectrum is obtained from the 3D one by applying the selection function and the full-treatment projection. Deviations from linear theory are already evident at $\ell \sim 40$.

For equilateral configurations where $\ell_1 = \ell_2 = \ell_3 = \ell$ we have:

in a) $C_\ell^3 \left[6 + 9 \sum_{mm'} \left(\begin{smallmatrix}\ell & \ell & \ell \\ m & -m & 0\end{smallmatrix}\right) \left(\begin{smallmatrix}\ell & \ell & \ell \\ m' & -m' & 0\end{smallmatrix}\right)\right]$ which, to a very good approximation, is $\simeq C_\ell^3 \left[6 + 9 \times 1.15/(2\ell+1)\right]$
in c) $9 B^2_{\ell\ell\ell}$

3.5 Likelihood analysis of a simulated catalogue

We created an all-sky catalogue with the APM selection function $\phi(r) \propto r^{-0.1} \exp[(-r/335)^2]$ (e.g. Maddox, Efstathiou & Sutherland (1995), Gaztanaga & Bernardeau (1998)), by replicating an N-body simulation of 500 Mpc h^{-1} side and then sparsely sampling and projecting to the plane of the sky 2303636 particles (galaxies for our purposes) accordingly to the APM selection function. The simulation was supplied by J. Peacock using the AP^{3}M code (Couchman 1991). The characteristics are: 128^3 particles, CDM transfer function (Bardeen et al. 1986), $\Gamma = 0.25$, $\Omega = 0.3$, $\Lambda = 0.7$, evolved to σ_8=1 to best fit the observed cluster abundance; this choice gives also a good fit to the COBE 4-year data (e.g. Tegmark 1996). The rate of sampling used ensures that the probability of selecting the same particle in the simulation more than once in the replicated box is negligible.

Figure 1 shows the angular power spectrum for the simulated projected catalogue. The solid line is the underlying power spectrum obtained from the 3D one by applying convolution with the selection function and full-treatment projection; the dashed line is the underlying linear power spectrum. Deviations for linear theory are already evident at $\ell \sim 40$. In order to lift the degeneracy between c_1 and c_2 we consider equilateral and degenerate configurations. The likelihood for equilateral configurations is shown in Figure 2; it does not give a strong constraint on the bias: perturbation theory breaks down at $\ell \sim 40$: up to $\ell < 40$ there are only 18 independent equilateral triplets[†]. The likelihood for degenerate configurations gives a better constraint on the bias. Perturbation theory for this configuration breaks down where the short ℓ is $\ell = 40$. Likelihood contours for degenerate triplets configurations where the short ℓ is $20 < \ell \leq 40$, are shown in Figure 3. Since the likelihood for equilateral configurations is quite broad, even combining it to the likelihood for degenerate configurations does not modify Figure 3 sensibly.

From this analysis we can conclude that from a two-dimensional galaxy survey with the APM selection function, even if it is an all-sky survey, it is only possible to constrain a combination of the linear and quadratic bias parameter, or, alternatively, if we *assume* (without justification) that the bias is linear (i.e. $b_2 = 0$), $0.7 < c_1 < 1.4$ or $0.7 < b_1 < 1.4$, at 68% confidence.

[†] 18 is the number of independent D_α as defined in eq. 35 with $\ell_i = \ell < 40$, $i = 1, 2, 3$. The presence of the 3-J symbol for equilateral configurations requires ℓ to be even, $\ell = 2$ is discarded because it would be contaminated by the galaxy quadrupole.

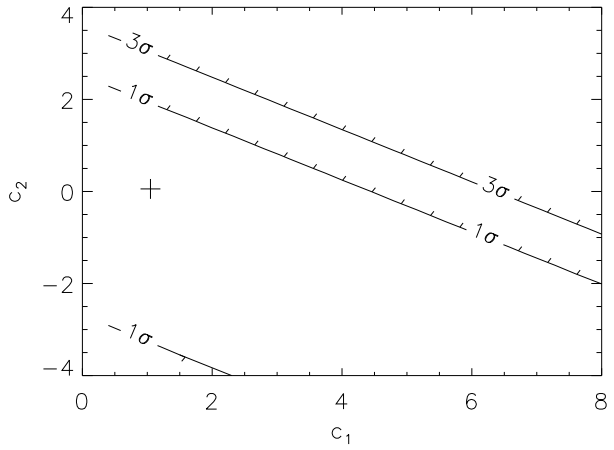

Figure 2. Likelihood contours for equilateral triplets configurations. The two levels (where the downhill direction is indicated for clarity) are the $1-\sigma$ and 3-σ confidence levels and the + indicates where the true value for the parameters lies. Perturbation theory breaks down at $\ell \sim 40$ here ℓ up to 42 are considered even though the likelihood only for the triplets between $\ell = 40$ and $\ell = 42$ includes the true value just within the boundary of the $3-\sigma$ level. This configuration does not place strong constraints on the bias parameter.

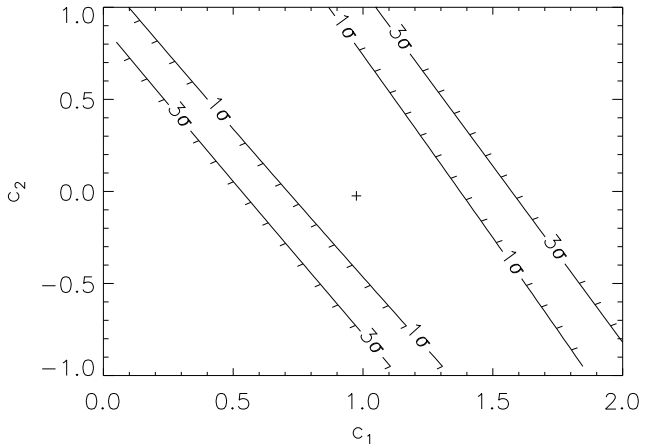

Figure 3. Likelihood contours for degenerate triplets configurations. The two levels are the $1-\sigma$ and 3-σ confidence levels and the + indicates where the true value for the parameters lies. Perturbation theory breaks down at $\ell_{\rm short} = 40$.

4 CONCLUSIONS

In this paper, we have presented the formalism for translating the 3D bispectrum of a sample population into the angular bispectrum in spherical harmonics. As discussed in section 2.1, this method has applications in a variety of areas, such as microwave background studies, gravitational lensing and analysis of angular galaxy catalogues. We have investigated the last of these in detail in this paper: since the bispectrum is a measurable quantity, and its theoretical expression depends on measurable quantities via the unknown bias parameter, it is possible to extract the bias parameter via a likelihood analysis. We have therefore investigated its use as a tool for measuring the bias parameter for projected galaxy surveys. In principle, it is an alternative method to using 3D galaxy redshift surveys, without the complicating effects of redshift distortions and higher shot noise. Recently, other methods based on second-order perturbation theory have been proposed to measure the bias parameter from 2D galaxy catalogues (see e.g. Frieman & Gaztanaga 1999; Fry & Thomas 1999). Frieman & Gaztanaga (1999) studied the reduced 3-point correlation function on the sky. The error analysis in real space is more complicated because of strong correlations between the estimates. Frieman & Gaztanaga conclude that $b_1 \ll 1.5$ or so, giving a comparable error to

our analysis (section 3.5) if b_2 is assumed to be zero. We emphasize that allowing a non-zero quadratic bias term opens up a wide range of acceptable linear bias parameters.

The analysis of Fry & Thomas (1999) is closest to ours. They consider the bispectrum, but present results in the small-angle approximation only. They do go some way in writing down the general expression for the angular bispectrum in spherical harmonics in terms of the 3D bispectrum. In this paper, by expanding the (general) dependence of the 3D bispectrum on angle between wavevectors in Legendre polynomials, we were able to derive a practical general relationship which is computable with few numerical integrations.

We have calculated the expected error on the linear bias parameter from an all-sky catalogue with a selection function similar to the APM survey. We find that the results are not encouraging for projected catalogues, and that it is preferable to undertake a bispectrum study of 3D galaxy redshift surveys such as the AAT 2dF or the Sloan Digital Sky Survey, using the methods discussed in MVH97 and Verde et al. (1998). Tests on simulated projected catalogues confirm our analytic findings. In a similar way as for 3D surveys (see discussion in MVH97), one can reduce the errors by subdividing the sky [‡], but by modest factors which do not change this basic conclusion, and at the expense of considerable complication in the analysis through window convolutions.

ACKNOWLEDGMENTS

LV acknowledges the support of a TMR grant. We thank John Peacock for providing the N-body simulation, Marc Kamionkowski, Ari Buchalter, Silvia Mollerach and Andy Taylor for useful discussions and the anonymous referee for helpful comments.

REFERENCES

Bardeen J. M., Bond J. R., Kaiser N., Szalay A. S., 1986. ApJ, 304, 15.
Baugh C., Efstathiou G.P., 1993. MNRAS, 265, 145.
Baugh C., Efstathiou G.P., 1994. MNRAS, 267, 323.
Bernardeau F., van Waerbeke L., Mellier Y., 1997. MNRAS, 290, 655.
Bharadwaj S., 1999. ApJ, 516, 507.
Buchalter A., Kamionkowski M., Jaffe A., 1999. ApJ, astro-ph/9903486.
Catelan P., Lucchin F., Matarrese S., Moscardini L., 1995. MNRAS, 276, 39.
Catelan P., Lucchin F., Matarrese S., Porciani C., 1998, MNRAS, 297, 692
Cen R. Y., Ostriker J. P., 1992. ApJ(Lett), 399, L13.
Colless M., 1996. In *proceedings of the Heron Island Conference*, http://msowww.anu.edu.au/heron/Colless/colless.html.
Colless M., 1999. In *'Redshift Surveys and Cosmology', Coral Sea Cosmology Conference II, Dunk Island*, http://www.mso.anu.edu.au/DunkIsland/Proceedings/Colless.
Cooray A., Hu W. ,1999, preprint, astro-ph/9910397
Couchman H. M. P., 1991. ApJ(Lett), 368, L23.
Dekel A., Lahav O., 1999. ApJ, 520, 24.
Djorgovski S. G., Gal R. R., Odewahn S. C., de Carvalho R. R., Brunner R., Longo G., Scaramella R., 1998. In: *Wide Field Surveys in Cosmology, 14th IAP meeting held May 26-30, 1998, Paris*, Editions Frontieres. p. 89.
Efstathiou G., Bond J. R., White S. D. M., 1992. MNRAS, 258, 1.
Falk T., Rangarajan R., Srednicki M., 1993. Apj(Lett), 403, 1.
Ferreira P. G., Magueijo J., Gorski K. M., 1998. ApJLett, 503, 1.
Frieman J. A., Gaztanaga E., 1999. ApJ, 521, L83
Fry J. N., Thomas D., 1999. astro-ph/9909212.
Fry J. N., 1984. ApJ, 279, 499.
Fry J. N., 1994. Phys. Rev. Lett., 73, No 2, 215.
Gangui A., Mollerach S., 1996. Phys. Rev. D, 54, 4750
Gangui A., Martin J., 200. MNRAS, astroph/9908009

[‡] The procedure of subdivision to increase the S/N appears counter-intuitive. In fact, nothing more is gained by this than by relaxing the precise shape of the triangles. It is easiest to demonstrate this in Fourier space in 3D. MVH97 considered the bispectrum $B(\mathbf{k}_1, \mathbf{k}_2, \mathbf{k}_3)$ and demonstrated that the S/N increases $\propto N^{1/2}$, where N is the number of subvolumes. Alternatively, in increasing the volume by a factor N, one has more triangles to analyse. MVH97's analysis includes the density of $\mathbf{k}_1$ states; relaxing the triangle shape configuration increases the number of $\mathbf{k}_2$ states by the ratio of the density of states (i.e. N). $\mathbf{k}_3$ is fixed at $-\mathbf{k}_1 - \mathbf{k}_2$, so the number of triangles for given $\mathbf{k_1}$ is $\propto N$, giving the same increase of S/N (see Verde 2000). In practice correlations may modify the details. This argument is a variant of that in Press et al. (1992).

Gangui A., Martin J., 2000. Phys. Rev. D submitted, astroph/0001361
Gangui A., Lucchin F., Matarrese S., Mollerach S., 1994. ApJ, 430, 447.
Gaztanaga E., Bernardeau F., 1998. A& A, 331, 829.
Gradshteyn I. S., Ryzhik I. M., 1965. *Table of Integrals, series and products*, editor A. Jeffrey, Academic Press.
Gunn J. E., 1995. In: *American Astronomical Society Meeting*, 4405.
Heavens A. F., Matarrese S., Verde L., 1998. MNRAS, 301, 797.
Heavens A. F., 1998. MNRAS, 299, 805.
Heavens A. F., 2000. in preparation.
Kaiser N., 1992. ApJ, 388, 272.
Kamionkowski M., Buchalter A., 1999, ApJ, 514, 7.
Loveday J., Efstathiou G., Peterson B. A., Maddox S. J., 1992. ApJ(Lett), 400, L43.
Loveday J., 1996. MNRAS, 278, 1025.
Luo X., 1994. ApJ(Lett), 427, 71.
Luo X., Schramm D. N., 1994. Phys. Rev. Lett., 71, 1124.
Maddox S. J., Efstathiou G. ,Sutherland W., *The APM Galaxy Survey III: an Analysis of Systematic Errors in the Angular Correlation Function and Cosmological Implications*, 1995.Technical Report, OUAST/95/32 Nuclear and Astrophysics Lab.
Maddox S. J., Efstathiou G., Sutherland W. J., Loveday J., 1990. MNRAS, 243, 692.
Matarrese S., Verde L., Heavens A., 1997. MNRAS, 290, 651.
Matsubara T., 1999. ApJ, 525, 543.
Mollerach S., Gangui A.,Lucchin F., Matarrese S., 1995. ApJ, 453, 1.
Mollerach S., Matarrese S., 1997. Phys. Rev. D, 56, 4494.
Muciaccia P. F., Natali P., Vittorio N., 1997. ApJ(Lett), 488, 63.
Munshi D., preprint, astro-ph/0001240.
Munshi D., Souradeep T., Starobinsky A. A., 1995. ApJ, 454, 552
Press W. H., Teukolsky S. A., Vetterling W. T., Flannery B. P., 1992. *Numerical recipes in Fortran, 2nd edition*, C.U.P., Cambridge.
Refriger A., Spergel D. N., Herbig T., 1998. ApJ astro-ph/9806349
Rees M. J., Sciama D. N., 1968. Nature, 519, 611.
Sachs R. K., Wolfe A. M., 1967. ApJ, 147, 73.
Scoccimarro R., Couchman H. M. P., Frieman J. A., 1999. ApJ, 517, 531.
Sobelman R. B., 1979. *Atomic Spectra and Radiative Transitions*, Springer-Verlag.
Somerville R. S., Lemson G., Sigad Y., Dekel A., Kauffmann G., White S. D. M., 1999, MNRAS, submitted, astro-ph/9912073.
Goldberg D. M., Spergel D. N., 1999. astro-ph/9811251.
Spergel D. N., Goldberg D. M., 1999. astro-ph/ 9811252.
Scoccimarro R., Colombi S., Fry J. N., Frieman J. A., Hivon E., Melott A., 1998, ApJ, 496, 586
Sunyaev R. A., Zel'dovich Y. B., 1980. MNRAS, 190, 413
Taruya A., Koyama K., Soda J., 1999. ApJ, 510, 541.
Tegmark M., Bromley B. C., 1999. ApJ(Lett), 518, 69.
Tegmark, M. 1996, ApJ Lett, 464, 35
Verde L., Heavens A., Matarrese S., Moscardini L., 1998. MNRAS, 300, 747.
Verde et al. 2000, in preparation.
Verde L. 2000, Phd Thesis, University of Edinburgh.
Wang L., Kamionkowski M., 1999, ApJ in press, astro-ph/9907431.

APPENDIX A: SPHERICAL HARMONICS

Spherical harmonics are the natural basis for describing a two-dimensional random field on the sky. The definition we use here is expressed in terms of the associate Legendre functions $P_\ell^m(\cos\theta)$:

$$Y_\ell^m(\Omega) \equiv Y_\ell^m(\theta,\phi) = \sqrt{\frac{(2\ell+1)(\ell-m)!}{4\pi(\ell+m)!}} P_\ell^m(\cos\theta) e^{im\phi} \times \begin{cases} (-1)^m \text{ for } m \geq 0 \\ 1 \text{ for } m < 0 \end{cases} \tag{40}$$

where ℓ and m are integers and $\ell \geq 0$, $-\ell < m < \ell$. Their orthogonality relation is:

$$\int_{4\pi} d\Omega Y_{\ell_1}^{m_1}(\Omega) Y_{\ell_2}^{*m_2}(\Omega) = \delta^K_{\ell_1\ell_2}\delta^K_{m_1m_2}. \tag{41}$$

Any two dimensional pattern $f(\Omega)$ on the surface of a sphere can be expanded as:

$$f(\Omega) = \sum_{\ell m} a_\ell^m Y_\ell^{m*}(\Omega) \tag{42}$$

where

$$a_\ell^m = \int d\Omega Y_\ell^m(\Omega) f(\Omega). \tag{43}$$

Useful relations involving the spherical harmonics are:

$$Y_\ell^{m*}(\Omega) = (-1)^m Y_\ell^{-m}(\Omega) \ , \ Y_\ell^m(-\Omega) = (-1)^{m+\ell} Y_\ell^m(\Omega). \tag{44}$$

and the identities:

$$\sum_{\ell m} Y_\ell^{*m}(\Omega) Y_\ell^m(\Omega') = \delta(\Omega - \Omega') \tag{45}$$

$$\exp(i\mathbf{k}\cdot\mathbf{r}) = 4\pi \sum_{\ell m} i^\ell j_\ell(kr) Y_\ell^{*m}(\Omega_\mathbf{k}) Y_\ell^m(\Omega_\mathbf{r}) \tag{46}$$

$$P_\ell(\cos\theta) = \frac{4\pi}{2\ell+1} \sum_{m=-\ell}^{\ell} Y_\ell^m(\Omega_\mathbf{r}) Y_\ell^{*m}(\Omega_\mathbf{k}) \tag{47}$$

where θ denotes the angle between the vectors $\mathbf{r}$ and $\mathbf{k}$. The latter is the addition theorem for spherical harmonics.

APPENDIX B: THE POWER SPECTRUM AND THE SMALL-ANGLE APPROXIMATION

The power spectrum of a 2-D distribution on the plane on the sky is given by the set of C_ℓ defined as:

$$\langle a_\ell^m a_{\ell'}^{m'*} \rangle = C_\ell \delta^K_{\ell\ell'} \delta^K_{mm'}. \tag{48}$$

The corresponding angular two-point correlation function can be expanded as

$$C(\theta) = \frac{1}{4\pi} \sum_\ell (2\ell+1) C_\ell P_\ell(\cos\theta) \tag{49}$$

with inverse relation is:

$$C_\ell = 2\pi \int_{-1}^{1} C(\theta) P_\ell(\cos\theta) d\cos(\theta) \tag{50}$$

On the other hand, for a plane two-dimensional distribution with power spectrum $P_{2D}(\kappa)$ the two-point correlation function is:

$$w(\theta) = \frac{1}{(2\pi)^2} \int P_{2D}(\kappa) \exp(i\boldsymbol{\kappa}\cdot\boldsymbol{\theta}) d^2\kappa = \frac{1}{(2\pi)^2} \int_0^\infty \int_0^{2\pi} P_{2D}(\kappa) \cos(\kappa\theta\cos\phi) d\phi \kappa d\kappa = \frac{1}{(2\pi)} \int_0^\infty P_{2D}(\kappa) J_0(\kappa\theta) \kappa d\kappa \tag{51}$$

In the small angle approximation, i.e. in equation (49) for small θ, we have that $P_\ell(\cos\theta) \sim J_0[(\ell+1/2)\theta]$, but, since small angular patches restrict us to high ℓ, $P_\ell(\cos\theta) \sim J_0(\ell\theta)$. We can therefore conclude that in the small-angle approximation

$$\ell \longrightarrow \kappa \ ; \quad C_\ell \longrightarrow P_{2D}(\ell) \tag{52}$$

For a real angular catalogue the two-dimensional galaxy density in the sky is obtained as follow. Let the true three-dimensional galaxy density field be $\rho(\mathbf{r})$ and the selection function be $\psi(r)$, normalized here to $\int dr r^2 \psi(r) = 1$. It is straightforward to obtain an expression for the angular power spectrum given the three-dimensional one:

$$\langle a_{\ell_1}^{m_1} a_{\ell_2}^{m_2 *} \rangle = \begin{cases} \frac{1}{n^2} \frac{2}{\pi} \int dk k^2 P(k) \left[\int dr r^2 \psi(r) j_{\ell_1}(k_1 r) \right]^2 & \text{if } m_1 = -m_2 \text{ and } \ell_1 = \ell_2 \\ 0 & \text{otherwise} \end{cases} \tag{53}$$

In the small-angle approximation this is (Kaiser 1992, Buchalter, Kamionkowski & Jaffe 1999):

$$P_{2D}(\kappa) = \int_0^\infty dr P_{3D}(\kappa/r) \psi^2(r) r^2 \tag{54}$$

Also in the presence of the selection function we can check that mapping (52) is valid and we can asses the limit of validity for the small angle approximation for the power spectrum.

Assuming the APM selection function $\phi(r) \propto r^{-0.1} \exp[(-r/335)^2]$, and a CDM power spectrum (Efstathiou, Bond & White 1992) with $\Gamma = 0.25$, we compared the angular power spectrum obtained with the exact projection as in equation (53) and with the small angle approximation [equation 54]. The result is shown in Figure 3: the small angle approximation introduces an error smaller than 3% for $\ell > 20$.

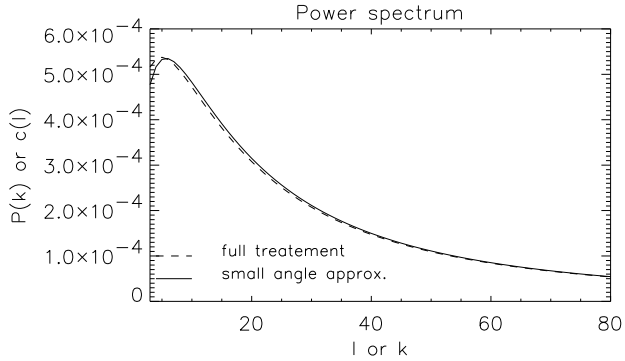

Figure 4. The small-angle approximation for the angular power spectrum works very well for $\ell > 20$ introducing an error smaller that 3%.

APPENDIX C: USEFUL FORMULAE FOR THE HIGH ℓ REGIME.

Library routines dealing with spherical harmonics at high ℓ can sometimes fail. In this appendix, we present some asymptotic results which can avoid problems.

The 3J symbol $\left(\begin{smallmatrix}\ell_1 & \ell_2 & \ell_3\\ 0 & 0 & 0\end{smallmatrix}\right)$ may be written as:

$$\left(\begin{smallmatrix}\ell_1 & \ell_2 & \ell_3\\ 0 & 0 & 0\end{smallmatrix}\right) = (-1)^L \sqrt{\frac{(L-2\ell_1)!(L-2\ell_2)!(L-2\ell_3)!}{(L+1)!}} \frac{(L/2)!}{(L/2-\ell_1)!(L/2-\ell_2)!(L/2-\ell_3)!} \tag{55}$$

where $L = \ell_1 + \ell_2 + \ell_3$.

In the special case where $\ell_1 = \ell_2 = \ell$ and $\ell_3 = 2\ell$ this becomes:

$$\frac{2[\Gamma(2\ell)]^2}{\sqrt{\ell}\sqrt{1+4\ell}[\Gamma(\ell)]^2\sqrt{\Gamma(4\ell)}} \tag{56}$$

Numerical routines to calculate the 3J symbols usually encounter problems for large ℓ. We therefore evaluated an approximation based on the Stirling approximation: i.e. $n! = \Gamma(n+1)$ and (Gradshteyn & Ryzhik 1965)

$$\Gamma(z) \sim e^{-z} z^{z-1/2} (2\pi)^{1/2} \quad \text{for large} \quad z. \tag{57}$$

This approximation for the Γ function is quite good, in fact it introduces an error of only 4% at $z = 2$. Using this approximation we obtain for eq. (55):

$$\left(\begin{smallmatrix}\ell_1 & \ell_2 & \ell_3\\ 0 & 0 & 0\end{smallmatrix}\right) \longrightarrow \frac{(-1)^{L/2}}{\sqrt{2\pi}} \frac{2^{1/4}\sqrt{e}}{(L+1)^{L/2+1/2+1/4}} \frac{L^{L/2+1/2}}{[(L/2-\ell_1)(L/2-\ell_2)(L/2-\ell_3)]^{1/4}}. \tag{58}$$

This approximation introduces a small error of a few percent at $\ell \sim 20$. For equation (56) we obtain:

$$\left(\begin{smallmatrix}\ell & \ell & 2\ell\\ 0 & 0 & 0\end{smallmatrix}\right) \longrightarrow \frac{1}{\sqrt{1+4\ell}} \left(\frac{4}{\ell 2\pi}\right)^{0.25} \tag{59}$$

When the m's are non-zero it is still possible to find a simple expression for the 3J symbol in special cases. For example if $\ell_3 = \ell_1 + \ell_2$ we have:

$$\left(\begin{smallmatrix}\ell_1 & \ell_2 & \ell_1+\ell_2\\ m_1 & m_2 & -m_1-m_2\end{smallmatrix}\right) = (-1)^{\ell_1-\ell_2+m_1+m_2} \sqrt{\frac{(2\ell_1)!(2\ell_2)!(\ell_1+\ell_2+m_1+m_2)!(\ell_1+\ell_2-m_1-m_2)!}{(2\ell_1+2\ell_2+1)!(\ell_1+m_1)!(\ell_2+m_2)!(\ell_1-m_1)!(\ell_2-m_2)!}} \tag{60}$$

In the special case where $\ell_1 = \ell_2 = \ell$ the previous expression can be further simplified and approximated –using (57)– by:

$$\left(\begin{smallmatrix}\ell & \ell & 2\ell\\ m_1 & m_2 & -m_1-m_2\end{smallmatrix}\right) \longrightarrow (-1)^{m_1+m_2} \frac{(\ell 2\pi)^{1/4}}{2^{2\ell}\sqrt{4\ell+1}} \sqrt{\frac{(2\ell+m_1+m_2)!(2\ell-m_1-m_2)!}{(l+m_1)!(\ell+m_2)!(\ell-m_1)!(\ell-m_2)!}} \tag{61}$$

In the calculation of the covariance matrix for "degenerate"configurations for the quantities $B_{\ell\ell 2\ell}$ we came across with the following sum over m of a product of two 3J-symbols. An useful expression for it is the following:

$$\sum_{m_1,m_2} \begin{pmatrix} \ell & \ell & 2\ell \\ m_1 & -m_1 & 0 \end{pmatrix} \begin{pmatrix} \ell & \ell & 2\ell \\ m_2 & -m_2 & 0 \end{pmatrix} = \frac{2^{(2+4\ell)}\ell^3\Gamma(2\ell)^4}{(1+4\ell)\Gamma(4\ell)\Gamma(2\ell+1)^2} \equiv \frac{2^{4\ell}\ell[(2\ell-1)!]^2}{(1+4\ell)(4\ell-1)!}. \tag{62}$$

For large ℓ using the above approximation for the Gamma function we obtain:

$$\frac{2^{4\ell}\ell[\Gamma(2\ell)]^2}{(1+4\ell)\Gamma(4\ell)} \longrightarrow \frac{\sqrt{2\pi}\sqrt{\ell}}{(1+4\ell)} \text{ (for large } \ell) \tag{63}$$

this approximation works very well also at low ℓ, in fact introduces an error below 1% at $\ell = 6$.

The orthogonality relations for 3J-symbols are also widely used:

$$\sum_{m_1\ m_2\ m_3} \begin{pmatrix} \ell_1 & \ell_2 & \ell_3 \\ m1 & m2 & m3 \end{pmatrix}^2 = 1 \tag{64}$$

and

$$\sum_{m_1\ m_2} \begin{pmatrix} \ell_1 & \ell_2 & \ell_3 \\ m1 & m2 & m3 \end{pmatrix} \begin{pmatrix} \ell_1 & \ell_2 & \ell_4 \\ m1 & m2 & m4 \end{pmatrix} = \frac{1}{(2\ell_3+1)} \delta^K_{\ell_3\ \ell_4} \delta^K_{m_3\ m_4} \tag{65}$$

When calculating the spherical harmonic coefficients for a galaxy distribution on the celestial sphere, numerical problems arise with the associate Legendre polynomials at high ℓ. Routines based on the recurrence relations used for example by the numerical recipes routines (Press et al. 1992) fails at $\ell \sim 35$ if $m \sim \ell$, at slightly higher ℓ for $m \ll l$. The asymptotic expansion for the associate Legendre polynomial (e.g.Gradshteyn & Ryzhik 1965):

$$P_\ell^m(\cos\theta) \simeq \frac{2}{\sqrt{\pi}} \frac{\Gamma(\ell+m+1)}{\Gamma(\ell+3/2)} \frac{\cos[(\ell+1/2)\theta - \pi/4 + m\pi/2]}{\sqrt{2\sin\theta}} + \mathcal{O}(1/\ell) \tag{66}$$

is valid for $\mid \ell \mid \gg \mid m \mid$, $\mid \ell \mid \gg 1$ and $\epsilon < \theta < \pi - \epsilon$.

The use of the recursive relations involve the calculation of $(2\ell-1)!!$ that at high ℓ can create numerical problems. Using the following expression for the Γ function:

$$\Gamma(n+1/2) = \frac{\sqrt{\pi}}{2^n}(2n-1)!! \tag{67}$$

and (57) for the Γ function for big argument we obtain:

$$(2n-1)!! = \frac{2^{n+1/2}(n+1/2)^n}{e^{n+1/2}} \tag{68}$$

This approximation introduces an error of only a few percent for $n \sim 10$.

When calculating the spherical harmonics at higher ℓ, problems arise not only with the associated Legendre polynomials, but also with the part that involves the ratio of two factorials. A better way to calculate the spherical harmonics, fast and accurate to high ℓ is based on the algorithm proposed by (Muciaccia, Natali & Vittorio 1997). In essence the numerical problems can be avoided by defining the normalized associated Legendre polynomials λ_ℓ^m:

$$\lambda_\ell^m(\cos\theta) \equiv \sqrt{\frac{2\ell+1}{4\pi}\frac{(\ell-m)!}{(\ell+m)!}} P_\ell^m(\cos\theta) \tag{69}$$

The recurrence relation for λ_ℓ^m is:

$$\lambda_\ell^m(x) = \left[x\lambda_{\ell-1}^m(x) - \sqrt{\frac{(\ell+m-1)(\ell-m-1)}{(2\ell-3)(2\ell-1)}} \lambda_{\ell-2}^m(x) \right] \sqrt{\frac{4\ell^2-1}{\ell^2-m^2}} \tag{70}$$

with expressions for the starting values:

$$\lambda_m^m(x) = (-1)^m \sqrt{\frac{2m+1}{4\pi}} \frac{(2m-1)!!}{\sqrt{(2m)!}} (1-x)^{m/2} \tag{71}$$

$$\lambda_{m+1}^m(x) = x\sqrt{2m+3}\lambda_m^m(x) \tag{72}$$

numerical evaluation can be greatly speeded up by noticing that the factor in (71) depends only on m and can therefore be calculated and/or tabulated for $m \leq \ell_{max}$ only once.